

Phase evolution in gel-precipitated LaAlO₃ ceramics

[Journal of Physics and Chemistry of Solids](#)

[Volume 69, Issue 8, August 2008, Pages 2041-2046](#)

<http://dx.doi.org/10.1016/j.jpcs.2008.02.019>

Archived in Dspace@nitr

<http://dspace.nitrkl.ac.in/dspace>

Phase evolution in gel-precipitated LaAlO₃ ceramics

Shantanu K. Behera*, Prashant K. Sahu, Swadesh K. Pratihari, Santanu Bhattacharyya

Department of Ceramic Engineering, National Institute of Technology, Rourkela 769008, India

ARTICLE INFO

Article history:

Received 12 January 2008

Received in revised form

20 February 2008

Accepted 28 February 2008

Keywords:

A. Oxides

B. Chemical synthesis

C. Infrared spectroscopy

C. Thermogravimetric analysis (TGA)

C. X-ray diffraction

ABSTRACT

Lanthanum aluminate ceramic powders could be prepared by a combined gel precipitation process from metal chlorides using ammonia. A slight modification in the conventional gel precipitation technique was carried out by introducing a step of ultrasonication followed by centrifugal washing of the gel. The dried gels produced pure phase lanthanum aluminate powders on calcination at 1100 °C for the combined gel-precipitated powders, and at 600 °C for the washed gel. The phase evolution was studied and it was found that the delay in obtaining monophasic LaAlO₃ in the combined gel-precipitated powder owed to the crystallization of an impure phase LaOCl. This phase was not detected in the washed gel (WG) powders. TEM micrographs showed a uniform morphology for the calcined WG powders, which were in contrast to the irregular particles in the gel-precipitated (GP) powders. The uniform morphology was assigned to the ultrasonic effects during washing of the gel.

1. Introduction

Lanthanum aluminate (hereafter referred to as LA) ceramics offer a desirable combination of properties like high-quality factor, high dielectric constant and zero temperature coefficient of resonant frequency, and are regarded as potential materials for microwave dielectric applications [1]. Single-crystal LA is used as substrate for depositing superconducting thin films because of its excellent lattice and thermal expansion matching with 1-2-3 superconductors [2]. LA has been prepared through various conventional routes like firing La₂O₃ and Al₂O₃ at higher temperatures [3], grinding La₂O₃ and transition alumina in high-energy ball mills [4] and advanced synthesis routes like co-precipitation of hydroxides [5–7], aerolising mixed metal nitrate solution into droplets and then pyrolysing them to evaporate the carrier solution [8], self-propagating high-temperature synthesis using urea and metal nitrate solution [9], auto-ignition of polyvinyl alcohol (PVA) solution and metal nitrate solution [10], pyrolysis of citric acid and metal nitrate solutions [11] and sol-gel synthesis [12]. While the mixed oxide routes pose several drawbacks like high reaction temperature, limited chemical homogeneity, large particle size, etc., the chemical routes have been proved to be extremely expensive due to the use of expensive precursors and sophisticated techniques without signifi-

cant improvement in the powder characteristics. Combined gel precipitation process has been applied to ceramic systems in the authors' laboratory for synthesis of fine powders with improved sinterability [13–15]. This method essentially combines precipitation and gelation. In this process, the concentration of the starting solution is increased to such an extent that during gelation process, when the gel becomes fully viscous, a substantial amount of the starting solutes still remains unreacted and it permeates through the gel network [13–15]. A similar procedure is followed in the present study, to synthesize LA from the chloride salts of La and Al. It is well known for systems with chloride precursors that the removal of chlorides from the synthesized powders is difficult. Separate batches of the gel have been prepared by combined gelation. An additional step of ultrasonication and centrifugal washing of the gel is employed for one batch. The phase evolution of LA in both the processes has been studied.

Few workers have reported the use of ultrasonics in separation of phases in clay-water systems [16]. However, in this investigation, ultrasonication was used for washing the combined gel. Ultrasonic energy is a form of mechanical vibratory energy propagating through materials media of all states. During its propagation high elastic forces are generated. Because of its high frequency, it can cause material failure and disruption. In a mixture of different phases such as gel and water, the inertial forces are very high, which break the surface tension and promote separation of phases. Ultrasonic energy is used to break the agglomerated particles, thereby producing an intimate and homogenous mixing. Thus, it enhances the possibility of reaction between the metal ions at a lower temperature. The present investigation is aimed at disseminating some of these effects.

* Corresponding author presently at: Center for Advanced Materials and Nanotechnology, Lehigh University, Bethlehem, PA 18015, USA.

Tel.: +1 610 758 3842; fax: +1 610 758 3526.

E-mail address: Behera@lehigh.edu (S.K. Behera).

2. Experimental

2.1. Materials synthesis

The powders synthesis flow diagram is outlined in Fig. 1. LaCl_3 (IRE, India) and AlCl_3 (E-merck, India) were used as precursors to produce 0.5M solutions of each cation in separate beakers by mixing with doubly distilled water. Then these two solutions were mixed in equimolar ratio and the resulting solution was magnetically stirred to get a uniform sol of the two cations. Ammonia solution (E-merck, India) was used as the precipitant. Dropwise addition of ammonia at first resulted in globule-like precipitates that gradually aggregated to form a continuous network structure throughout the whole volume of the original solution, thereby ceasing the stirring action of the magnetic bar. The gel was oven dried at 110°C for 24 h. The porous, fluffy and fragile dried gel was ground to fine powders, henceforth referred to as gel precipitated (GP) powders. In another sequence, excess ammonia was added even after gelling was complete and the precipitated gel structure was disrupted ultrasonically. The ultrasonicated gel was centrifugally washed at 6000 rpm for 10 min, followed by redispersing the precipitate in distilled water with ultrasonication. The presence of chloride ion was tested with AgNO_3 solution after each washing. Centrifugal washing was repeated 5–6 times for each batch till the filtrate produced clear solution with AgNO_3 . The washed mass was then dried overnight to get another batch of porous fluffy mass. The dried mass was ground to a fine powder, hereafter referred to as washed gel (WG) powders. Further LaCl_3 solution of 0.5M, taken in a beaker, was gelled by dropwise addition of ammonia that resulted in $\text{La}(\text{OH})_3$ gel. A similar procedure was followed for obtaining $\text{Al}(\text{OH})_3$ gel starting with AlCl_3 solution. Both the gels were oven dried and ground to obtain individual metal hydroxide gel powders.

2.2. Materials characterization

The chlorine content in the powders was analyzed by Water's Ion Chromatography (Model 632, USA) by digesting the powder samples using Schoninger combustion method to get a clear solution. In order to compare the effect of washing on chlorine ion removal, both the GP and WG powders, calcined at different temperatures, were analyzed. The thermal behavior of both GP and WG powders was studied from room temperature to 1000°C at a heating rate of $10^\circ\text{C min}^{-1}$ by a differential thermal analyzer (Model TG/DTA 32, Seiko, Japan). The phase analysis was done by powder X-ray diffraction method (Model PW 1730, Philips, Holland) using $\text{Cu-K}\alpha$ radiation ($\lambda = 1.54056 \text{ \AA}$) at an accelerating voltage of 30 kV, a current of 25 mA and a 2θ scan rate of $2^\circ/\text{min}$. The powder samples were mounted on a flat XRD plate and scanned at room temperature in the range $20^\circ\text{--}80^\circ$. Primary crystallite sizes of the powders were calculated from full-width at half-maximum (FWHM) values from the most intense peak of the diffractogram, the (112) reflection in this case, using Scherrer equation,

$$D = \frac{0.899\lambda}{\beta \cos \theta_B}$$

where D is the crystallite size (nm), λ is the wavelength of X-ray source (nm), β is the FWHM value (radians) and θ_B is the Bragg angle of the peak under consideration, i.e. the (112) reflection in this case. Photo acoustic infrared spectroscopy (PA-FTIR, Shimadzu IR-470 dispersive spectrophotometer) was performed on the as-synthesized and calcined powders to examine the chemical species present and their variation with different annealing conditions. The samples were diluted in a KBr matrix (1:200) and pressed pellets were scanned over the spectrum range $4000\text{--}400 \text{ cm}^{-1}$ and the spectra were averaged out from 64 scans with a nominal resolution of 2 cm^{-1} . A scanning electron microscope (Leica Stereoscan 440, LEICA, England) in secondary electron mode was used to analyze the particle/agglomerate size, morphology and the amount of agglomeration of the particles. The powder samples were dispersed with isopropanol and then a thin film of the alcoholic dispersion was deposited on a copper stub and dried. The samples were then sputter-coated with Au-Pd conductive coating before microscopy. Transmission electron microscopy (JEM 1200 EX, JEOL, Japan) was performed at an accelerating voltage of 100 kV by dispersing the samples ultrasonically in isopropanol and then depositing them on a polymer-coated copper grid. The particle/agglomerate size, morphology and the amount of agglomeration were studied using standard TEM settings.

3. Results and discussion

3.1. Chemical analysis

In the first method, the mixed solution of lanthanum and aluminum chloride is precipitated using NH_4OH as the destabilizing agent. In the lines of combined gel precipitation it may be expected that the gel contains hydroxides of the cations, i.e. $\text{La}(\text{OH})_3$ and $\text{Al}(\text{OH})_3$, NH_4Cl as the reaction products and unreacted solutes (AlCl_3 and LaCl_3) that are arrested in the gel structure. The microanalysis of both the powders at different calcination conditions are presented in Table 1. The GP powders showed 36% Cl content. The chlorine content in the GP powders, thus, can be assigned to the presence of NH_4Cl , AlCl_3 and LaCl_3 . Moreover, the microanalysis of the GP powders at 1100°C records 3.5% of Cl content, which may only be due to any chloride form of lanthanum as the chlorides of ammonium and aluminum are not

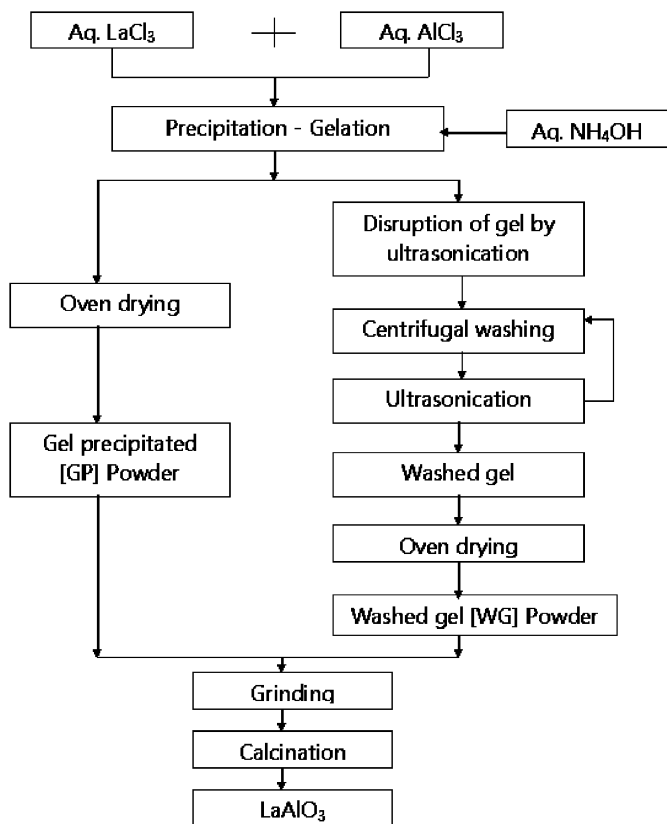


Fig. 1. Flow diagram of powder synthesis.

Table 1

Chlorine content of GP and WG powders at different temperatures

Conditions	GP powders (%)	WG powders
As-synthesized	36	2.5%
Calcined at 600 °C/4 h	4.25	0.12%
Calcined at 1100 °C/4 h	3.5	<0.1%
Calcined at 1300 °C/4 h	0.8	NA

stable at high temperatures. This suggests that the as-synthesized GP powder has a significant amount of entrapped LaCl_3 , which is not precipitated during gelation. The same logic could also be extended to the entrapment of AlCl_3 in the gel. In contrast, processing of the gel via the second process was carried out with an additional step of ultrasonication and centrifugal washing of the gel. Microanalysis of the dried powders showed a small amount of Cl (2.5%). The reduction in chlorine content in the second process might be due to the magnetic stirring followed by ultrasonication that might have disrupted the gel structure, and the immobilized unreacted solutes might have been precipitated by the addition of excess ammonia. The remaining NH_4Cl might have been separated from the system with repeated centrifugal washing.

The PA-FTIR studies are also in agreement with the micro-analysis of the powders. The important regions in the infrared spectra of the powders prepared by a combined gel precipitation are (i) $3300\text{--}3100\text{ cm}^{-1}$ region (assigned to the O–H and N–H with O–H occurring at higher wave numbers), (ii) $1630\text{--}1200\text{ cm}^{-1}$ region (assigned to the N–H stretching vibrations), (iii) $1200\text{--}800\text{ cm}^{-1}$ region (assigned to the –OH bending vibrations), and (iv) $900\text{--}400\text{ cm}^{-1}$ region (assigned mostly to the Al–OH and La–OH stretching vibrations) [17]. The FTIR plots of individual metal hydroxide gels are shown; Fig. 2(a) is the spectra of $\text{Al}(\text{OH})_3$ gel and Fig. 2(b) is that of $\text{La}(\text{OH})_3$ gel. In both the spectra, the broad absorption band at 3200 cm^{-1} region corresponds to the O–H stretching vibrations of the hydroxide gels [18]. A sharp peak is observed at 1400 cm^{-1} in the spectra of both the metal hydroxides, which is the characteristic absorption band of NH_4Cl [19]. This suggests the presence of NH_4Cl in both of the individual metal hydroxides. A series of small and diffused absorptions is observed in the $900\text{--}400\text{ cm}^{-1}$ region (Fig. 2a) which are due to the vibrations of Al–OH bonds in aluminum hydroxide. Over the same region in Fig. 2b two distinct absorption bands are observed at 700 and 550 cm^{-1} . These are characteristic La–OH bond vibrations in $\text{La}(\text{OH})_3$. The FTIR spectra of the GP powders (Fig. 2c) and WG powders (Fig. 2d) show absorption bands in the 3400 cm^{-1} region. This may be assigned to the vibrations of the –OH bonds in the stretching mode [18]. The spectra of the two powders, however, are different with respect to the 1400 cm^{-1} absorption. There is a clear absorption band at 1400 cm^{-1} in case of the GP powders, whereas the same peak for WG powders is very faint. This band corresponds to NH_4Cl . In addition, there are reasonably clear characteristic peaks of NH_4Cl in the $3000\text{--}2800\text{ cm}^{-1}$ ranges in the GP powders. Absorption in this region is absent in case of the WG powders. These observations suggest that the GP powders have a significant amount of NH_4Cl as against a small amount in WG powders. This is in close agreement with the results of elemental analysis of the powders. The broad absorption band centered at around 570 cm^{-1} in the GP as well as WG powders may be assigned to Al–OH and La–OH vibrations. The characteristic absorptions of neither the La–OH bonds nor the Al–OH bonds are observed in the GP and WG powders. Thus, it can be safely assumed that La and Al ions are homogeneously distributed in the gel powders, resulting in a broad single absorption in this region.

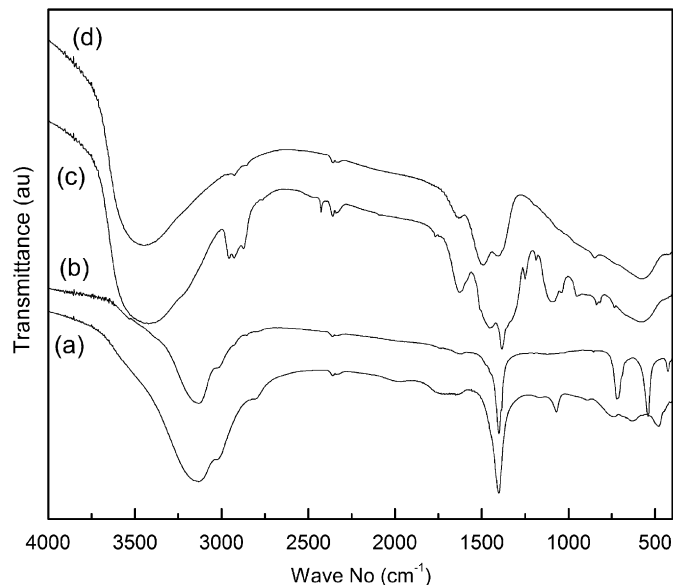


Fig. 2. PA-FTIR spectroscopy of as-synthesized powders (a) aluminum hydroxide gel, (b) lanthanum hydroxide gel, (c) GP powder and (d) WG powder.

The differences in the powder characteristics prepared by two almost identical synthesis routes underscore the importance of ultrasonication. Ultrasonic waves move about in three dimensions with successive cycles of compression and rarefaction. This results in cavitation, which is a burst of energy throughout the whole volume accompanied by a local increase in pressure and temperature [16]. These effects, presumably, are responsible for a difference in chlorine content in the powders prepared by two different processes. Cavitation is even more prominent in gel–water systems, which results in a separation of solid–liquid interface. In the present investigation, this may have expedited the separation of the gel from water thereby exposing the unreacted chlorides to precipitate in presence of excess ammonia. In addition to this, when the gel–water system is irradiated with ultrasonic waves, energy is absorbed and subsequently there is a rise in temperature. This causes a decrease in viscosity and the gel structure is broken, facilitating removal of chlorides to form hydroxides.

3.2. Thermal analysis

The DTA curves in Fig. 3 represent the decomposition behavior of the individual metal hydroxides. It can be seen that the decomposition of $\text{Al}(\text{OH})_3$ takes place in three stages (curve a, Fig. 3). The endothermic peak at 80 °C represents the loss of adsorbed moisture in the gel powders. The peak at 205 °C may be assigned to the loss of NH_4Cl from the system [14]. The subsequent endothermic peaks at 300 , 375 and 430 °C indicate the decomposition of $\text{Al}(\text{OH})_3$ to its amorphous oxide state. This is in close agreement with previously reported three stage decomposition of $\text{Al}(\text{OH})_3$ gels [14]. In contrast to this, the decomposition of $\text{La}(\text{OH})_3$ is a single-step process (curve b, Fig. 3). The peak at 190 °C may be the loss of NH_4Cl from the gel, similar to the loss pattern in $\text{Al}(\text{OH})_3$ gel. The large endothermic peak at 280 °C represents the conversion of $\text{La}(\text{OH})_3$ to amorphous La_2O_3 .

The thermal behavior of the individual hydroxides can be used to understand the relatively complex DTA trends of the GP and WG powders. The DTA of the GP powders (Fig. 4a) showed two distinct endothermic peaks with higher degree of endothermicity

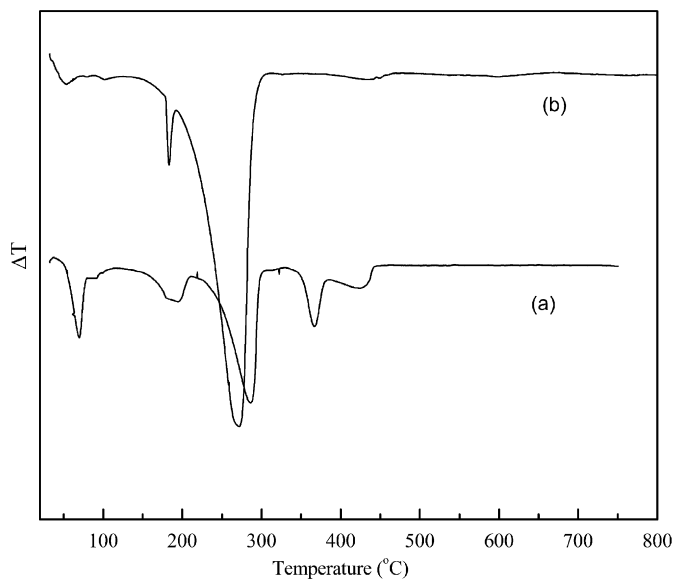


Fig. 3. DTA of individual metal hydroxide gels (a) Al-hydroxide gel and (b) La-hydroxide gel.

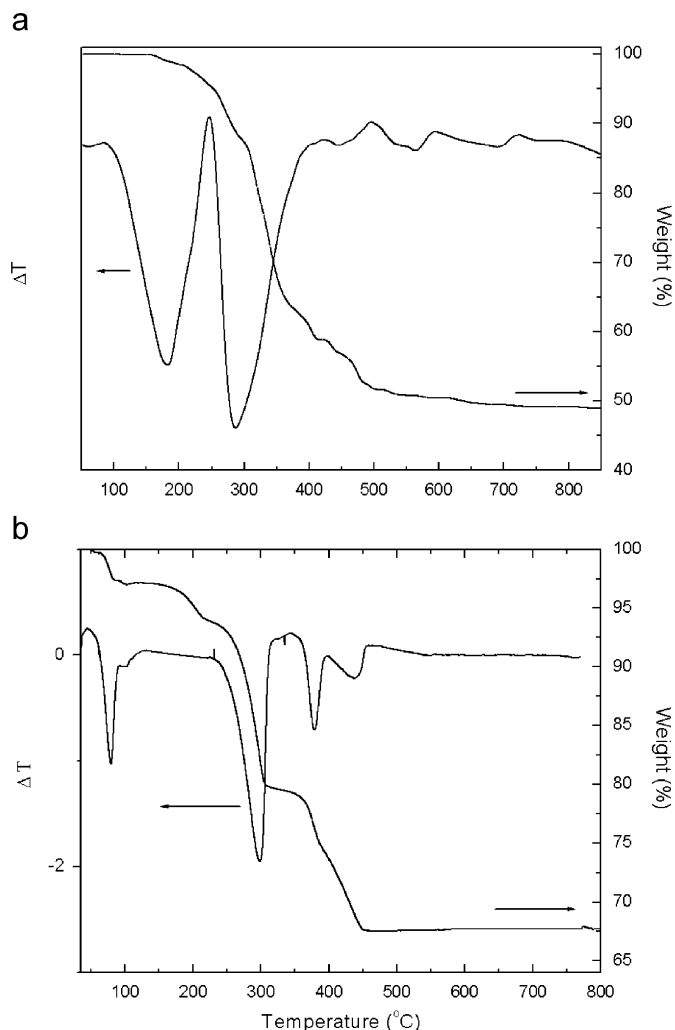


Fig. 4. (a) DTA and TGA plots of as-synthesized GP powders and (b) DTA and TGA plots of as-synthesized WG powders.

at 190 and 300 °C. The endothermic peak centering at 190 °C owes to the removal of a large amount of NH_4Cl present in the powders. The second endothermic peak, observed at 285 °C, includes the dehydroxylation of $\text{La}(\text{OH})_3$ as well as that of $\text{Al}(\text{OH})_3$. It may be noted that the successive stages of dehydroxylation normally observed for aluminum hydroxide gels is not observed here. However, the endothermic peak is observed over the same temperature range as the case was for aluminum hydroxide gel. Thus, the endothermic peak at 285 °C may be ascribed to the decomposition of $\text{La}(\text{OH})_3$ and the initial two stages of decomposition of $\text{Al}(\text{OH})_3$. Owing to the presence of so many phases in the GP powder, the thermal behavior of the gel becomes quite complex and, as all the endothermic reactions take place in a close temperature range, the individual reaction temperatures in the GP powders might have shifted slightly as compared to the temperatures in the thermal behavior of individual metal hydroxide powders. A small endothermic peak is observed at 450 °C, which may be due to the final stage of decomposition of $\text{Al}(\text{OH})_3$. The DTA of the WG powders (Fig. 4b) showed four distinct endothermic peaks. The peak at 80 °C may be due to the removal of moisture in the gel. No peak in the region of 200 °C is found in the WG powders (as against the peak in GP powders), which suggests that there are no NH_4Cl retained in the powders. This inference fits well with the results of elemental analysis and FTIR spectra of WG powders. The large endothermic peak at 300 °C may have accommodated two reactions: the decomposition of $\text{La}(\text{OH})_3$ to La_2O_3 as well as the first decomposition peak of $\text{Al}(\text{OH})_3$. The subsequent endothermic peaks at 375 and 430 °C represent the other two stages of $\text{Al}(\text{OH})_3$ decomposition. The reaction temperatures observed in the WG powders are quite similar to that of the individual metal hydroxide gels.

The thermo-gravimetric analysis (TGA) of the as-synthesized powders is in agreement with the DTA peaks showing distinct regimes of weight loss corresponding to the temperature regions mentioned in the DTA. The TGA of the GP powders shows a weight loss of more than 50% and most of it occurs below 500 °C with a faint weight loss continuing till higher temperatures. This large weight loss could be because of the dehydroxylation of hydroxides, conversion of metal chlorides into oxides as well as removal of excess NH_4Cl from the system. In contrast to this, TGA curve of the WG powder shows that there is a loss of 27% in weight for the WG powders and that the powders are loss free after 450 °C. The theoretical estimation of weight loss for conversion of lanthanum and aluminum hydroxides into respective oxides is 20%. As only 5% weight loss in TGA is due to the moisture present in the powders, it may be inferred that the weight loss over this temperature range is mainly due to the conversion of metal hydroxides to oxides. However, the small difference in weight loss between the theoretical estimation and experimental data could be due to the removal of chlorine from the powders.

3.3. Phase evolution and powder morphology

X-ray diffraction patterns of the as-synthesized GP powders (Fig. 5a) showed sharply defined peaks of NH_4Cl (ICDD File card no. 77-2352) indicating its presence in a significant amount [14]. On the contrary, the as-synthesized WG powders were amorphous and no distinct crystalline phase could be detected (Fig. 5b). In particular there are no peaks for any compounds, including chlorides and hydroxides of lanthanum and aluminum, found in both the powders (except NH_4Cl in GP powders). The diffractogram indicates that all such compounds may be present in the powders in an amorphous form. The GP powders calcined at 400 °C for 4 h showed crystallization peaks of LaOCl (ICDD File card no. 08-0477). The presence of chlorine in the system as LaCl_3

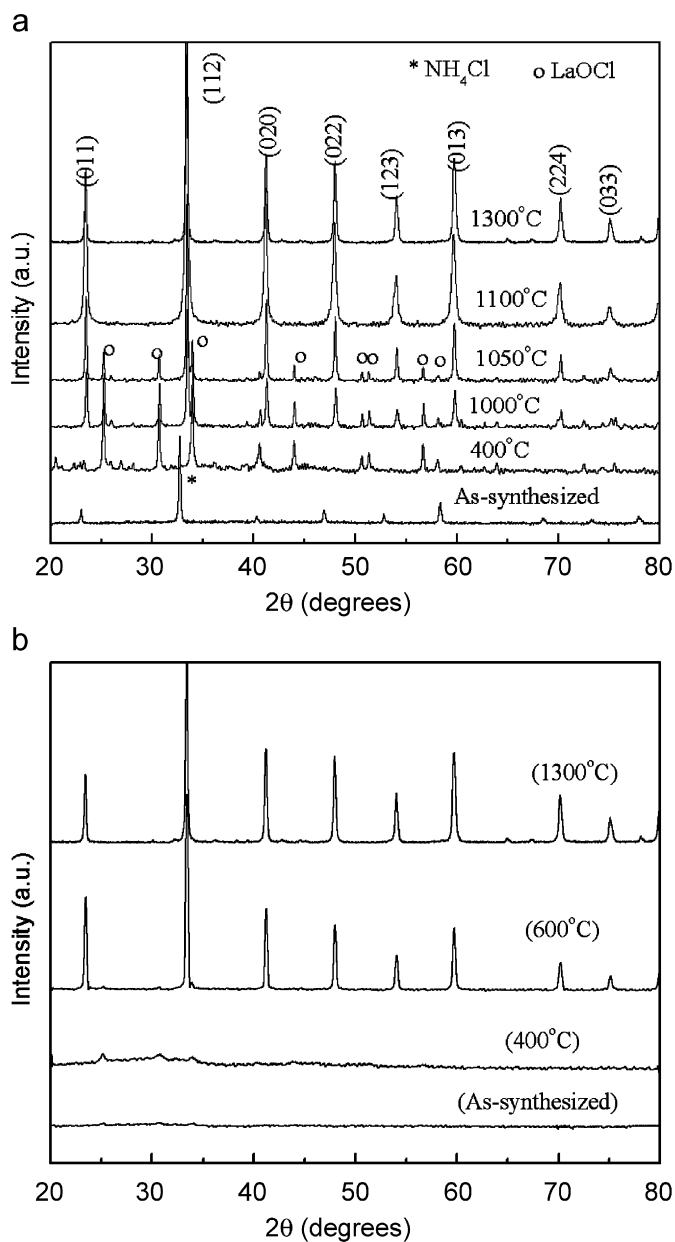


Fig. 5. (a) XRD pattern of GP powders calcined at different temperatures and (b) XRD pattern of WG powders calcined at different temperatures.

might have reacted with the amorphous La_2O_3 to form this phase. However, crystallization peaks of LA of rhombohedral symmetry could be observed for GP powders calcined at 600°C for 4 h, and the maximum peak in the diffractogram corresponded to the maximum peak position of crystalline LA (ICDD File card no. 31-0022). Calcination of the powder at higher temperatures (e.g. 800 , 1000 and 1050°C) still showed peaks of LaOCl along with the peaks for LA. However, the intensity of the LaOCl peaks gradually decreased on higher calcination temperatures and complete crystallization peaks of LA were observed in the samples calcined at 1100°C for 4 h. X-ray diffraction patterns of the WG powders, on the other hand, showed no clear peaks (Fig. 5b) confirming completely the amorphous nature of the powders. However, the same powders calcined at 600°C for 4 h showed complete crystallization peaks of LaAlO_3 , which could be indexed on rhombohedral symmetry. The calculated lattice parameters of both the crystallized powders ($a = 5.357 \text{ \AA}$, $\alpha = 60.1^\circ$,

$V = 108.951 \text{ \AA}^3$, and space group $R\text{-}3c$)¹ confirmed the theoretical values of LaAlO_3 perovskite [20]. In the present work, the crystalline LaAlO_3 phase may have evolved from a completely homogeneous mixture of the metal hydroxides in the precipitated gel, which may have brought down the crystallization temperature. The diffractograms of powders calcined at higher temperatures showed a gradual increase in their sharpness. Both the powders calcined at 1600°C , however, showed sharply defined LaAlO_3 peaks. This confirms that the powders prepared by both the routes are thermally stable up to 1600°C and that no second-phase formation takes place during the heat treatment process.

Combining all the experimental observations and results, we propose that the following chemical reactions may have occurred during phase evolution. In the GP powders, there is ample amount of chloride; so amorphous La_2O_3 may have reacted with chloride to form the LaOCl phase as per the following equation:



The presence of LaOCl peaks in X-ray diffractograms suggests that LaOCl is a very stable chloride in comparison with Al chlorides, and this may have delayed the LaAlO_3 phase formation. The decrease in intensity of LaOCl peaks in the diffractograms indicates the gradual disappearance of that phase. This may have occurred as per the following reaction:

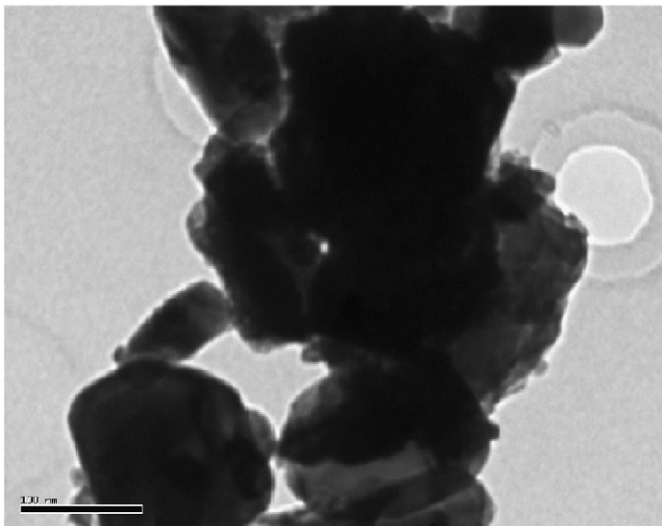


Though the system takes oxygen from the atmosphere, there is also a loss of 2 mol of chlorine for every mole of oxygen coming into the system. This is well supported by a small and continued weight loss at higher temperatures in the TGA curve (Fig. 4a). Later the amorphous oxides of aluminum and lanthanum react to form LA phase and at this stage no impure phase other than LA is retained in the system. The significant drop in crystallization temperature for the WG powders may be assigned to a few reasons. Combined gel precipitation process ensures a completely homogenous distribution of metal ions in the system to produce fine particles. However, fine particles spontaneously agglomerate in suspensions and by the process of ultrasonication the agglomerates in the precipitated gel are broken and individual particles are redispersed with improved uniformity. In addition, the absence of any chlorides prevents the formation of an impure phase so that LA forms directly from the loss-free metal hydroxides immediately after dehydroxylation. The high free energy of the amorphous oxides of lanthanum and aluminum may have expedited the crystallization of LaAlO_3 . On the other hand, the formation of phase pure LA gets delayed by the presence of an impure phase (LaOCl) in the GP powder.

The TEM micrograph of the GP powders (Fig. 6a) shows that the particles are of $80\text{--}100 \text{ nm}$ size. On the other hand, the TEM micrograph of the WG powders (Fig. 6b) shows up as spherical nanoparticles with sizes in the range of $25\text{--}40 \text{ nm}$. The crystallite sizes of both the powders were calculated from the peak broadening of X-ray diffractograms using Scherrer equation. The crystallite sizes were 32 and 50 nm for the GP powders calcined at 1100 and 1300°C , respectively. The WG powders showed sizes of 28 and 35 nm for similar calcination conditions. These numbers are consistent with the results obtained by direct visualization of particles through TEM. It may also be noted that TEM micrographs generally represent particle sizes, whereas the Scherrer equation gives an average value of the primary crystallite size. For the GP powders a factor of ~ 2 difference in the values obtained by X-ray and TEM studies indicates that the powder is slightly

¹ A phase transition of LaAlO_3 occurs at $435 [\pm 25]^\circ\text{C}$ from the high temperature cubic phase (space group $Pm\bar{3}m$) to the rhombohedral phase ($R\text{-}3c$).

a



b

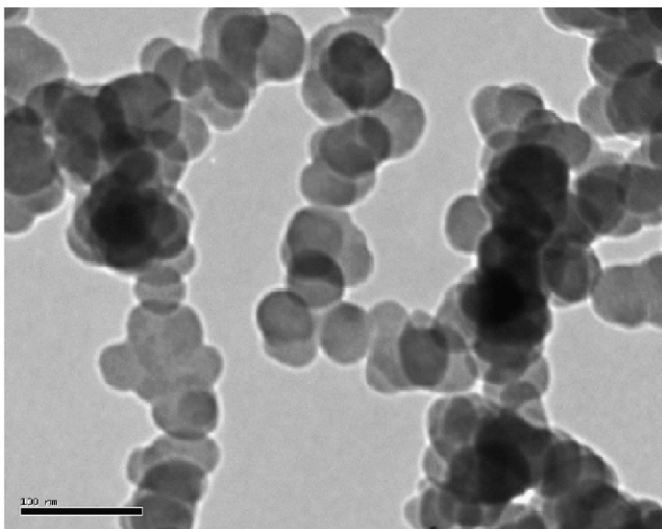


Fig. 6. (a) TEM micrographs of GP powders and (b) TEM micrographs of WG powders.

agglomerated and each particle is a cluster of primary crystallites. On the other hand, for the WG powders, values obtained from both the techniques were similar, indicating that the WG powders are essentially free of agglomeration. With regard to the morphology of the synthesized powders, it can be observed from the micrographs that the GP powders are highly irregular in shape. On the contrary, the WG powders are monodispersed in nature; the particles are fairly uniform and spherical in their morphology, fitting to a close size distribution range. The difference in particle morphology can be assigned again to

ultrasonic effects. With cavitation and associated local rise in temperature and pressure, the gel network is broken and the high amount of energy burst causes disruption of the agglomerates [15]. The disruption caused at the particle–water interface modifies the surface properties, leading to a change in particle morphology. The dispersion obtained from ultrasonic washing is so uniform that it produces phase pure LaAlO_3 nanopowders with a narrow size distribution at temperatures as low as 600°C .

4. Conclusion

Lanthanum aluminate ceramic powders could be prepared by combined gel synthesis with metal chlorides as precursors and NH_4OH as destabilizing agent. The first process showed the formation of LA at 600°C along with an impure phase of LaOCl . Phase pure LaAlO_3 could be obtained at a calcination temperature of 1100°C . In the second route, when the gel was redispersed by ultrasonication and centrifugally washed to remove the chlorides present, phase pure LaAlO_3 could be obtained at low temperature of 600°C . It may be inferred that the control of particle dispersion in suspension effectively improves the powder characteristics and reduces the phase formation temperature. The TEM micrographs of the WG powders, calcined at 600°C , show a fairly spherical morphology of the LaAlO_3 powders with size ~ 25 nm and narrow size distribution, whereas the calcined powders from the gel precipitation routes have been found to be polydispersed and irregular in their morphology.

References

- [1] S.-Y. Cho, I.-T. Kim, K.S. Hong, *J. Mater. Res.* 14 (1999) 114.
- [2] R.W. Simon, C.E. Platt, A.E. Lee, G.S. Lee, K.P. Daly, M.S. Wire, J.A. Luine, M. Urbanik, *Appl. Phys. Lett.* 53 (1988) 2677–2679.
- [3] M.L. Keith, R. Roy, *Am. Mineral.* 39 (1954) 1–23; G.Y. Sung, K.Y. Kang, S.C. Park, *J. Am. Ceram. Soc.* 74 (1991) 437–439.
- [4] Q. Zhang, F. Saito, *J. Am. Ceram. Soc.* 83 (2000) 439–441.
- [5] K. Vidyasagar, J. Gopalkrishnan, C.N.R. Rao, *J. Solid State Chem.* 58 (1985) 29–37.
- [6] A.M. Golub, T.N. Maidukova, T.F. Limar, *Izv. Akad. Nauk, Neorg. Mater.* 2 (1996) 1608–1611.
- [7] J. Nair, P. Nair, F. Mizukami, *J. Am. Ceram. Soc.* 83 (2000) 1942–1946.
- [8] B.C. Lux, R.D. Clark, A. Silazar, L.K. Sveum, M.A. Krebs, *J. Am. Ceram. Soc.* 76 (1993) 2669–2672.
- [9] E. Taspinar, A.C. Tas, *J. Am. Ceram. Soc.* 80 (1997) 133–141.
- [10] A.K. Adak, P. Pramanik, *Mater. Lett.* 30 (1997) 269–273.
- [11] M.D. Shajikumar, T.M. Srinivasan, C. Subramaniam, P. Ramasamy, *Mater. Lett.* 25 (1995) 171–174.
- [12] P. Peshev, V. Slavova, *Mater. Res. Bull.* 29 (1994) 255–261.
- [13] V.K. Singh, R.K. Sinha, *Mater. Lett.* 31 (1997) 281.
- [14] S. Bhattacharyya, S.K. Pratihari, R.K. Sinha, R.C. Behera, R.I. Ganguly, *Mater. Lett.* 53 (2002) 425–431.
- [15] S.K. Behera, P.K. Sahu, S.K. Pratihari, S. Bhattacharyya, *Mater. Lett.* 58 (2004) 3710–3715.
- [16] G. Onal, M. Ozer, F. Arslan, *Miner. Eng.* 16 (2003) 129–134.
- [17] C.B. Sawyer, J.S. Reed, *J. Am. Ceram. Soc.* 84 (6) (2001) 1241–1249.
- [18] D. Mishra, S. Anand, R.K. Panda, R.P. Das, *J. Am. Ceram. Soc.* 85 (2) (2002) 437–443.
- [19] D.A. Skoog, D.M. West, *Principles of Instrumental Analysis*, second ed., Saunders College, Philadelphia, 1980, p. 231, Tables 8–12.
- [20] S. Geller, V.B. Bala, *Acta Crystallogr.* 9 (1956) 1019–1025.